

Applied Data Science

Assignment 1

Declan Jackson
Student ID: 1080086

September 9, 2021

1 Question 1

1.1 Part 1

Figure 1 shows the plots for each standardised TC. If we normalised the data rather than standardised it, each value would be either 0 or 1. This would mean we would lose information about spread of the data. For example, in **TC₁** the data is centred around 0, meaning the TC vector's value is equally -1 and 1. For **TC₂** however, the data is centered around 0.25, which shows that the value of the **TC₂** vector is more likely to be 1 rather than 0. We therefore normalise rather than standardise to keep this information about different distributions within time courses.

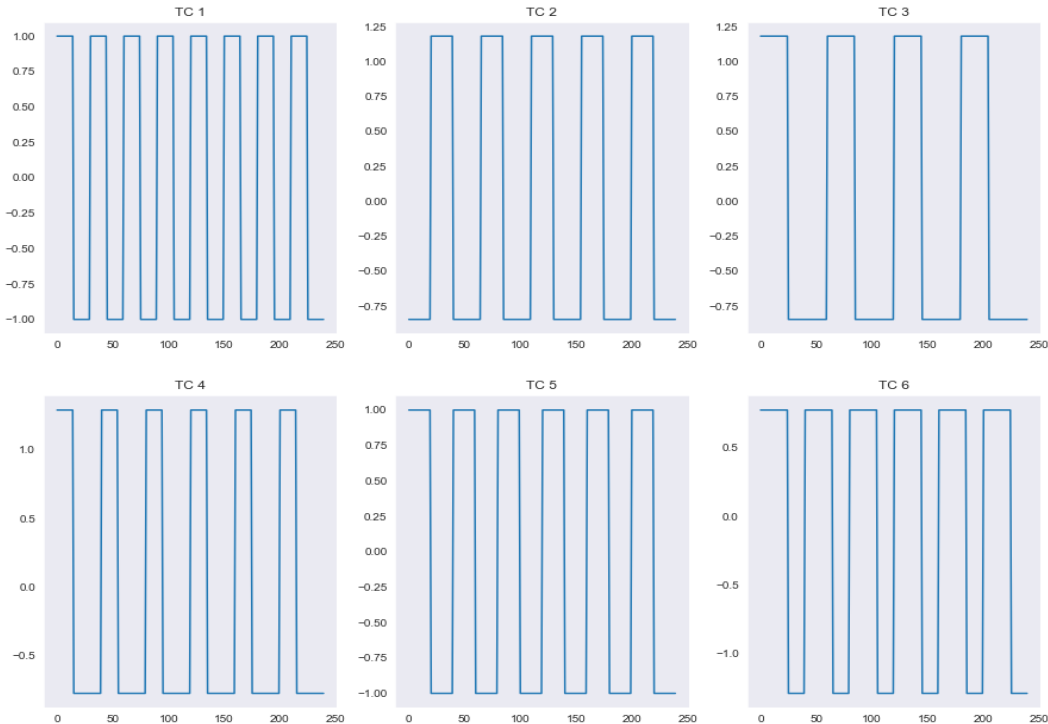


Figure 1: The six temporal sources making up matrix **TC**

1.2 Part 2

Looking at the plots in Figure 1, it can be deduced that time courses 4, 5 and 6 are all quite similar. When one of these time courses is at its maximum value, it is likely that the other time courses are at their peak as well. This is confirmed by the correlation matrix (CM) in Figure 2. This Figure shows that the highest correlation exists between \mathbf{TC}_4 and \mathbf{TC}_5 , and between \mathbf{TC}_5 and \mathbf{TC}_6 .

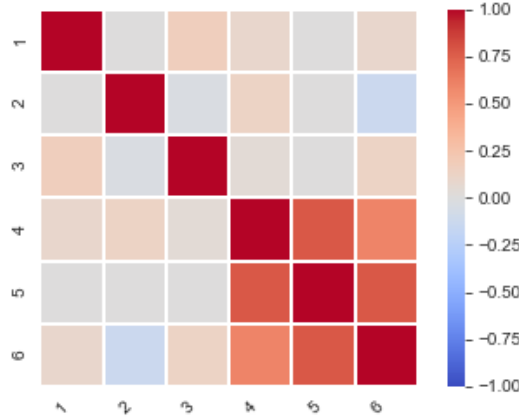


Figure 2: A CM representing the correlation between the 6 TC variables

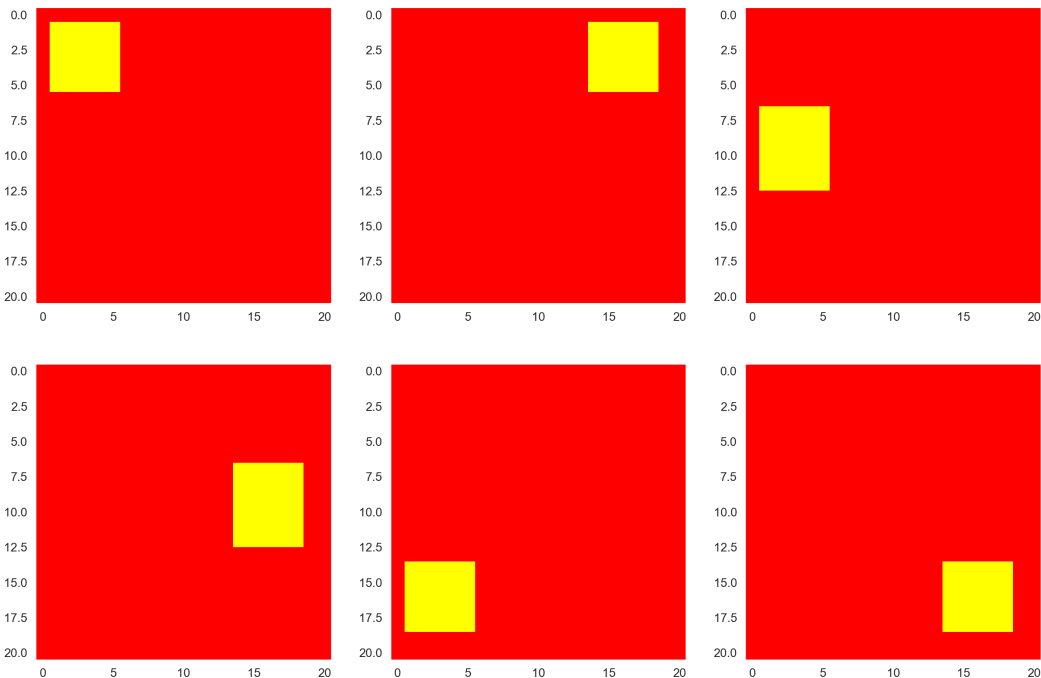


Figure 3: The six spatial map sources

1.3 Part 3

From the plots of each spatial map source in Figure 3, it can be seen that none of the areas where the temporal signal is activated in each plot overlaps with another plot. The independence is confirmed by Figure 4, which shows there is no correlation between any of the spacial map sources. There is no need to standardise the spatial maps, as opposed to the time courses. This is because it is important that the pixel values are either 0 or 1 in the theoretical model. This is because when we multiply **TC** by **SM** the values representing pixels that are not activated (i.e. SM value is 0) should also be 0. It must be noted however that this is only in the theoretical model, as it does not account for noise. Also, the data does not need to be standardised as it is simply communicating whether a given space is activated or not. If one of the slices had pixel values of 5, while others remained at one for instance, each slice would still equally communicate which spaces are activated, and the 5 would not give us any extra information.

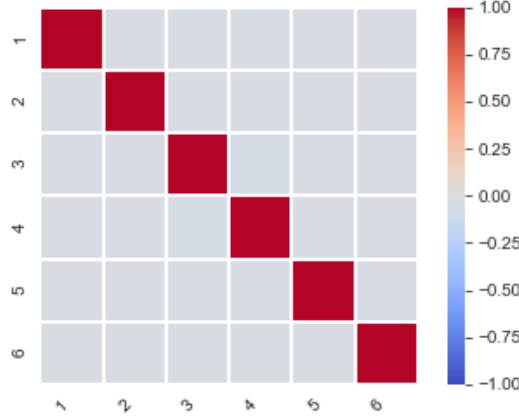


Figure 4: CM of the six spatial map sources

1.4 Part 4

From the CMs below (Figures 5 and 6), we can see that the white Gaussian noise for temporal and spatial sources is only slightly correlated between sources. Figures 7 and 8 show the distributions of the noise. The noise looks to be normally distributed for the most part, and this is confirmed by the sample mean and variances for the distributions (see table 1). This is also supported by the fact that close to 95% of the data in both cases is in the range $[-1.96\cdot\sigma, 1.96\cdot\sigma]$. The variables in the product $\Gamma_t \Gamma_s$ are very correlated. Figure 10 shows the number of V variables which have a certain level of correlation with at least one other variable in the data set. All 441 variables have a correlation of 0.7 with at least one other variable, and 6 variables have a correlation of at least 0.99 with at least one other variable. These variables are shown in figure 9, where it can be seen that this strong correlation is a mixture of positive and negative correlation.

Distribution	Sample Mean	Sample Variance	% of Data withing range $[-1.96\cdot\sigma, 1.96\cdot\sigma]$
Γ_t	-0.011	0.241	95.6%
Γ_s	-0.002	0.0143	94.7%

Table 1: Distribution statistics for Γ_t and Γ_s

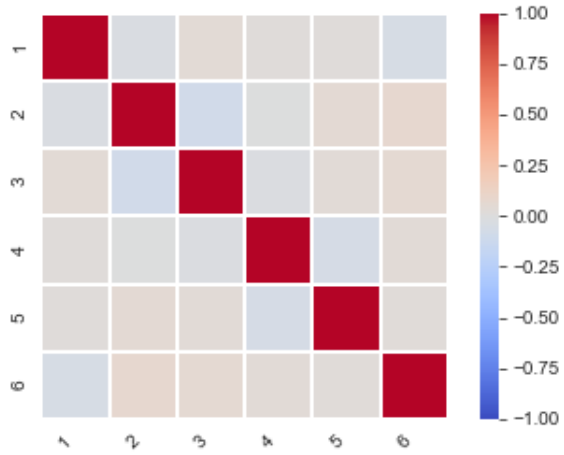


Figure 5: CM for Γ_t

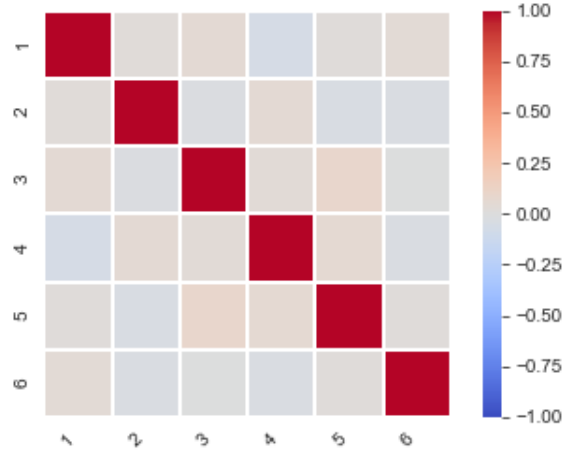


Figure 6: CM for Γ_s

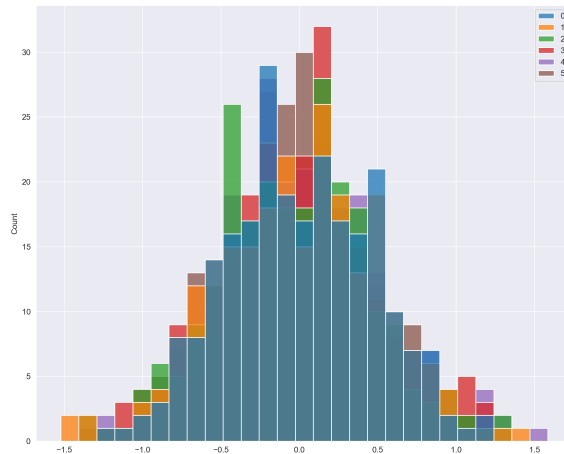


Figure 7: Distribution of Γ_t

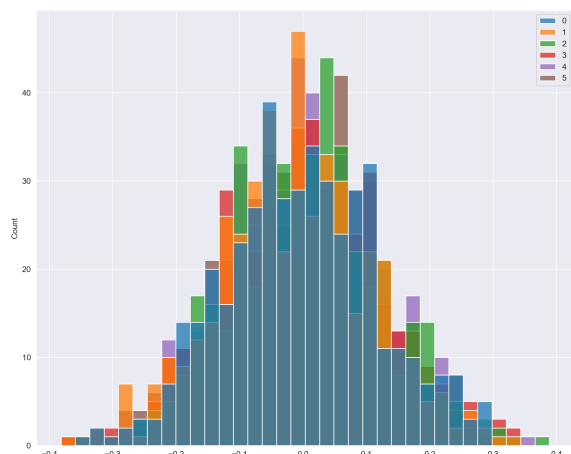


Figure 8: Distribution of Γ_s

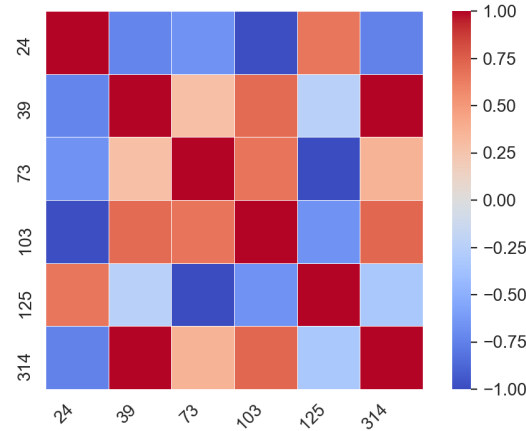


Figure 9: 6 variables with the strongest correlation to another variable

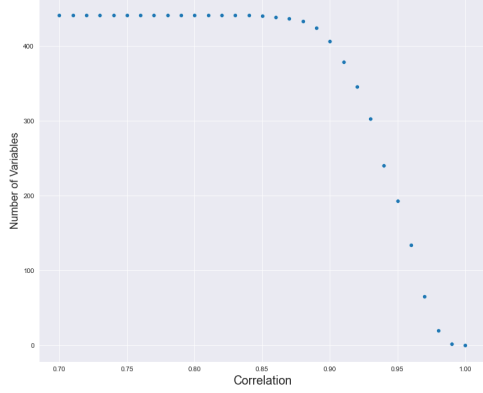


Figure 10: Number of variables with certain level of correlation with at least 1 other variable

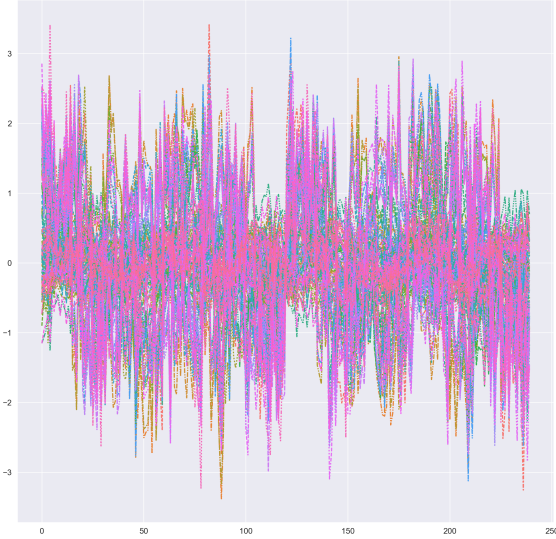


Figure 11: 100 of the variables from \mathbf{X}

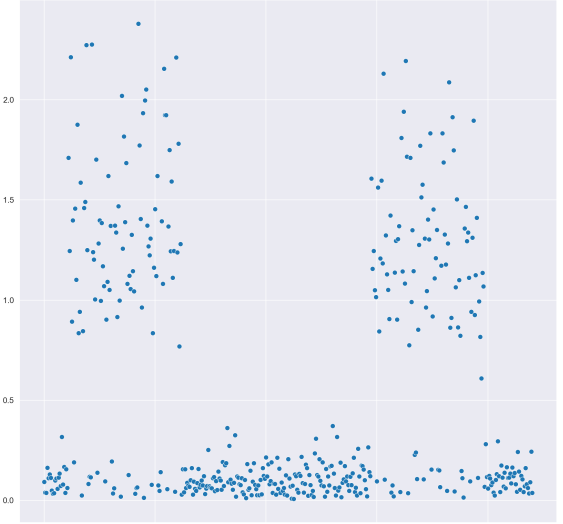


Figure 12: Variances of 441 variables in \mathbf{X}

1.5 Part 5

When expanding the \mathbf{X} matrix, we get the products $\mathbf{TC} \cdot \mathbf{SM}$, $\mathbf{TC} \cdot \Gamma_s$, $\Gamma_t \cdot \mathbf{SM}$, and $\Gamma_t \cdot \Gamma_s$. We know that the product $\mathbf{TC} \cdot \mathbf{SM}$ is represented by \mathbf{DA} in the linear model equation, and the product $\Gamma_t \cdot \Gamma_s$ is represented by \mathbf{E} . This leaves the remaining products $\mathbf{TC} \cdot \Gamma_s$ and $\Gamma_t \cdot \mathbf{SM}$. Since these are multiples of randomly generated variables with $\mu = 0$, the products also have an average value of 0. This means they are also part of the model error, and therefore part of \mathbf{E} in our final model. Figure 12 shows us the distribution of the variances of each column of \mathbf{X} . Each column of \mathbf{X} represents a pixel on the SMs, and therefore it is not surprising that there is an increase in variance around columns 30 to 100 and columns 300 to 400. This is because there is greater variance in those pixels as they take on the values 1 and 0. In each spatial map, we see the middle is always 0, which is why the pixels 100 to 300 have much lower variance. This variance is only due to the noise.

2 Question 2

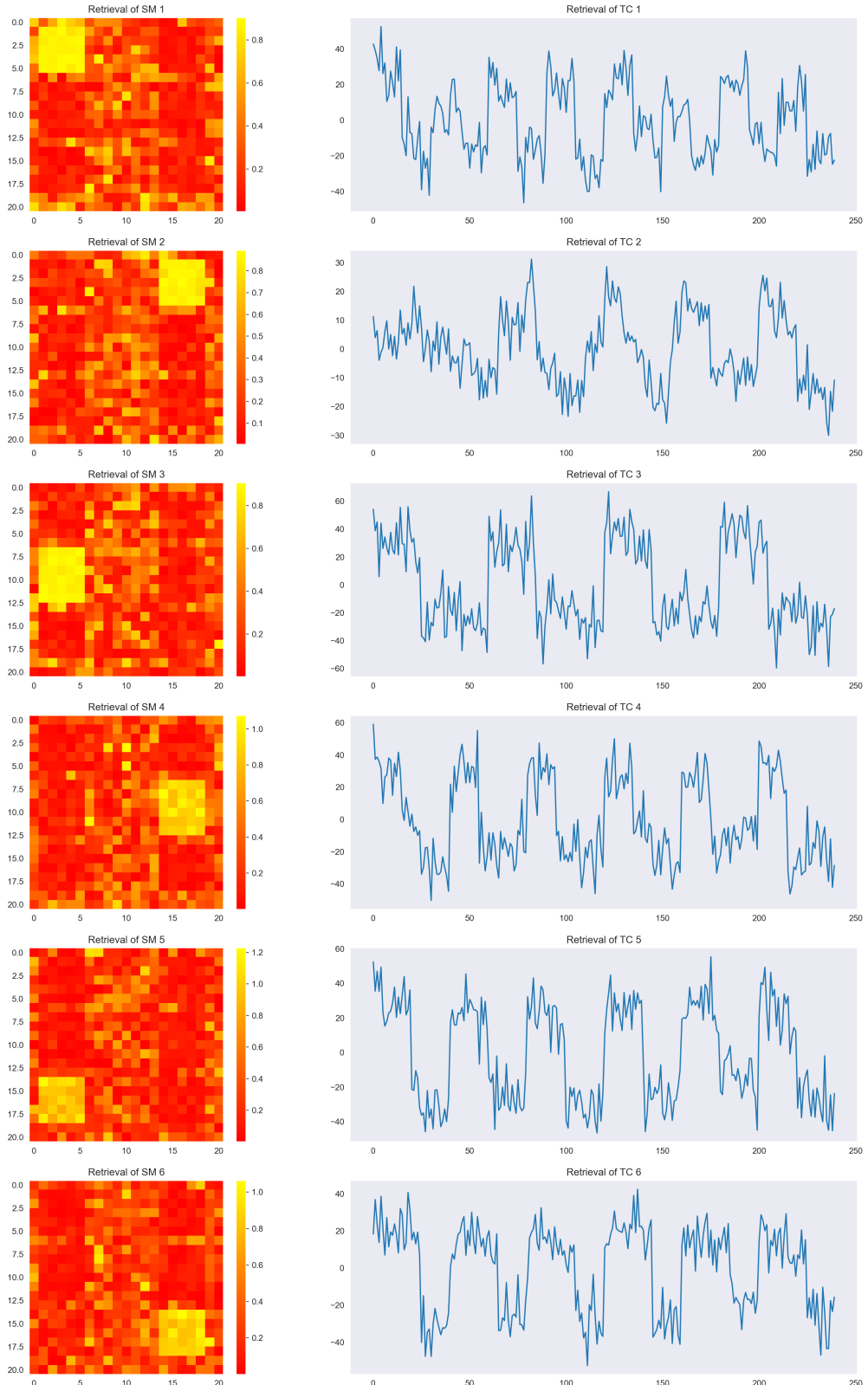


Figure 13: The 6 retrieved sources using least squares regression

2.1 Part 1

From Figure 14, we see a strong positive linear relationship between the 30th column of \mathbf{X} and the 3rd column of \mathbf{D}_{LSR} . The 30th column of \mathbf{X} represents the 9th pixel in the 2nd column of the spatial maps. The 3rd column of \mathbf{D}_{LSR} represents our retrieval of the 3rd column of \mathbf{TC} , the time course relating to the 3rd spatial map. The reason for the strong correlation is that the 9th pixel in the 2nd column of the 3rd spatial map is activated. This relationship is not present with any other column of \mathbf{D}_{LSR} as none of the spatial maps to which these time courses relate have their 30th pixel activated.

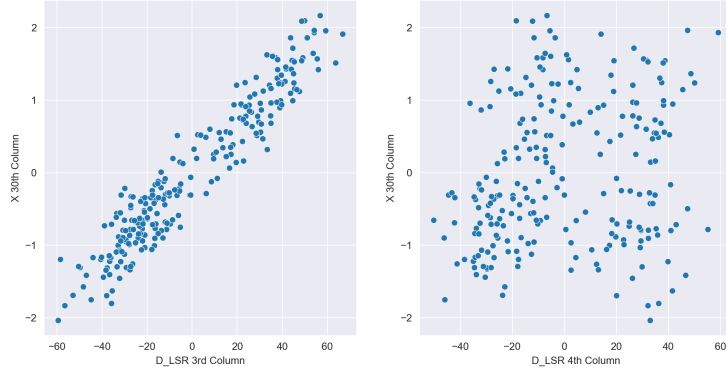


Figure 14: The relationships between the 30th column of \mathbf{X} and the 3rd and 4th column of \mathbf{D}_{LSR}

2.2 Part 2

Using a guess and check method to ensure that $\sum c_{TRR} > \sum c_{TLSR}$, $\lambda = 0.2$ was used for the Ridge Regression. The following values were obtained:

$$\sum c_{TRR} \approx 5.148 \text{ and } \sum c_{TLSR} \approx 5.138 \quad (1)$$

We can see below in Figure 15 that the overall relationship between predictors in \mathbf{A}_{LSR} and \mathbf{A}_{RR} is similar. The value of these predictors however is very different, as we see that the scale for the \mathbf{A}_{RR} values is much smaller, meaning that the values of the predictors has been shrunk a lot more than in the Ridge Regression as opposed to the Least Squares Regression. This is because we have increased λ to 1000, which means the effect of the Least Squares Regression in our Ridge Regression model is less significant, and co-efficients of the model are more heavily penalised and shrunk towards 0.

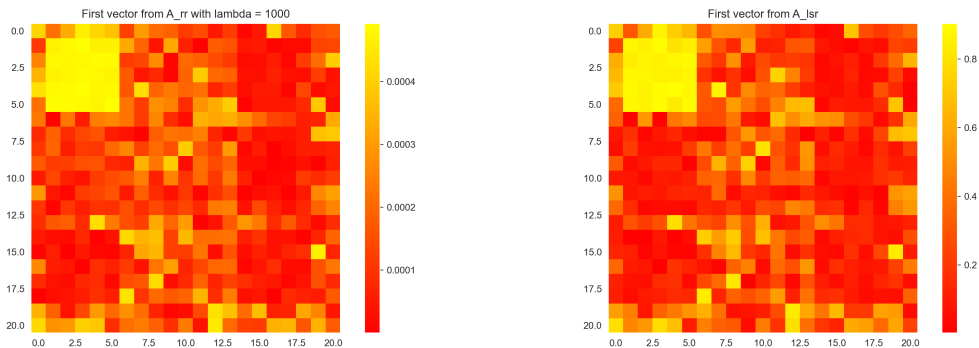


Figure 15: The first vector from \mathbf{A}_{RR} with $\lambda = 1000$, and the corresponding vector from \mathbf{A}_{LSR}

2.3 Part 3

The minimum MSE was found at the value $\rho = 0.6$. This is a suitable value to choose for ρ as it is not so large that it has shrunk all predictors to 0, but it is high enough to ensure that we have adequately fit our model. We could, however, consider using an elbow method approach and choose the value of ρ at which the MSE stops decreasing significantly. This would be if we wanted to ensure we keep most of our predictor variables whilst still obtaining a low MSE. The value of ρ started increasing again right after our optimal value ($\rho = 0.6$), and at $\rho = 0.95$, the MSE stayed at 1.0, suggesting that all of our variables have been shrunk very close to 0, or even removed.

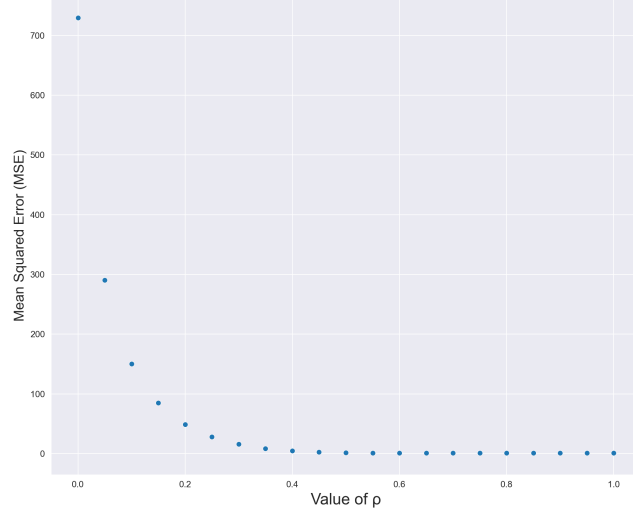


Figure 16: The Mean Squared Error for each value of ρ

2.4 Part 4

Using $\rho = 0.6$, we are able to calculate \mathbf{D}_{LR} and \mathbf{A}_{LR} with LASSO regression. The correlation results are below in Table 2. We can see that these results are as expected, as the relationships $\sum c_{TRLR} > \sum c_{TRRR}$ and $\sum c_{CSLR} > \sum c_{SRSS}$ hold. We can also see in Figure 17 that the Ridge Regression has many more false positives (yellow spots) in the retrieved spatial maps, compared to the LASSO regression. This is most likely due to Ridge Regression's penalisation term being a squared value, as opposed to an absolute value, like it is in LASSO. What this means is LASSO not only punishes high co-efficient values, but also removes them completely if they are not relevant. Ridge Regression on the other hand just shrinks these co-efficients to a small value, which may explain this high number of false positives. It must also be noted that the regularisation parameter for Ridge, λ , was not obtained by minimising the mean squared error, but found by simply using guess and check. This also may have contributed to the lack of accuracy in the retrievals using Ridge Regression.

Correlation Vector	Approximate Sum
c_{TRRR}	5.148
c_{SRSS}	3.577
c_{TRLR}	5.395
c_{CSLR}	5.032

Table 2: Correlation values between original data and retrieved data for Ridge and LASSO Regression

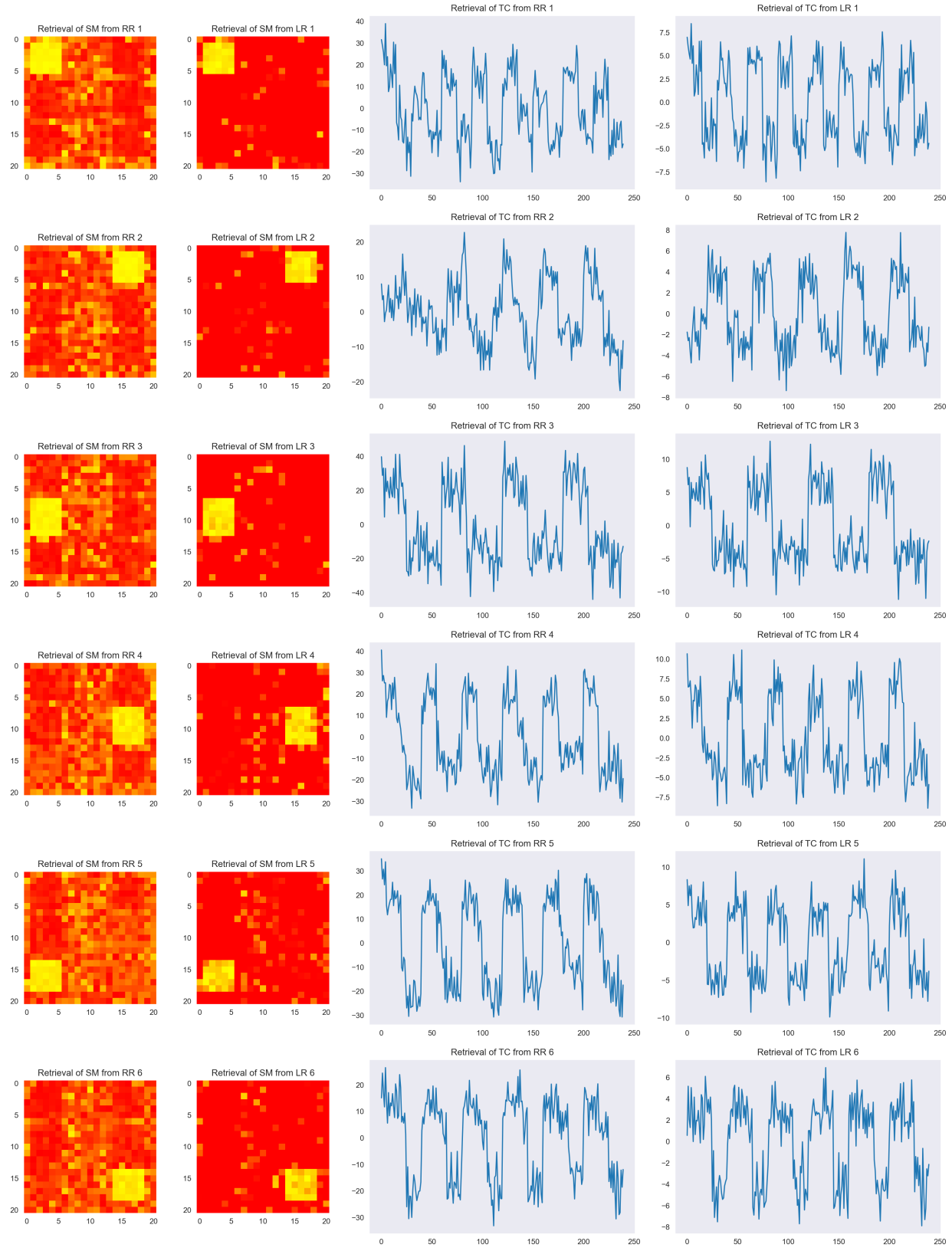


Figure 17: The 6 retrieved sources using Ridge Regression and LASSO Regression

2.5 Part 5

From Figure 18 we can see that the PC which has the smallest eigenvalue is the 5th principal component ($\lambda_5 \approx 0.154$). The PCs have little resemblance to the time courses (Figure 19). This is because the PCs are built from the eigenvectors of the covariance matrix, and hence they are orthogonal, unlike our original time courses which have high correlation (Figure 2). The PCs are also linear combinations of all of the TCs, and therefore we do not expect them to each resemble a specific TC. Using these PCs is not a good idea, as they are not reflective of our original data. This is confirmed in the poor results from our LASSO Regression using the PCs (Figure 20). The spatial maps are a strong visual indication of why the PCs should not be used as each retrieval reflects how each PC was a mixture of all the data. For instance, the retrieval of SM from PCA 2 looks to be mainly made up of vectors 1 and 3 from **SM**. The retrievals of the TCs also do not resemble the original data from **TC**. This is unsurprising as the matrix from which these retrievals were built, **Z**, does not bear resemblance to the original time courses.

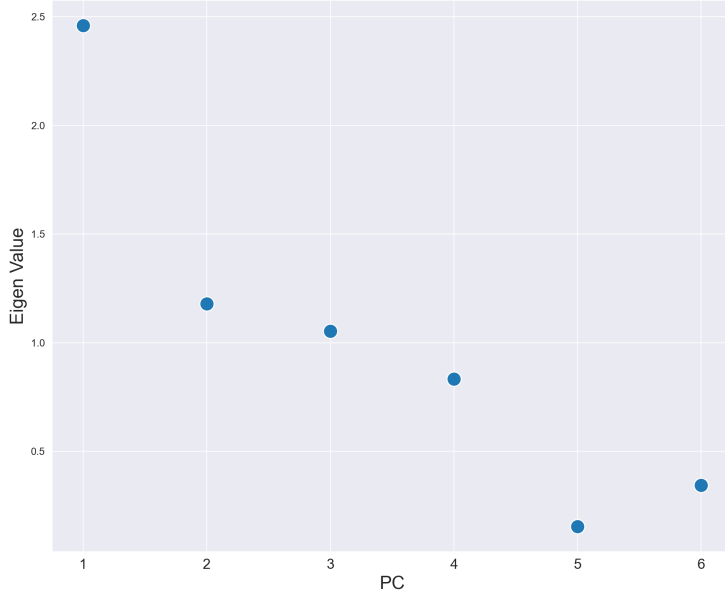


Figure 18: The eigenvalues of each principal component

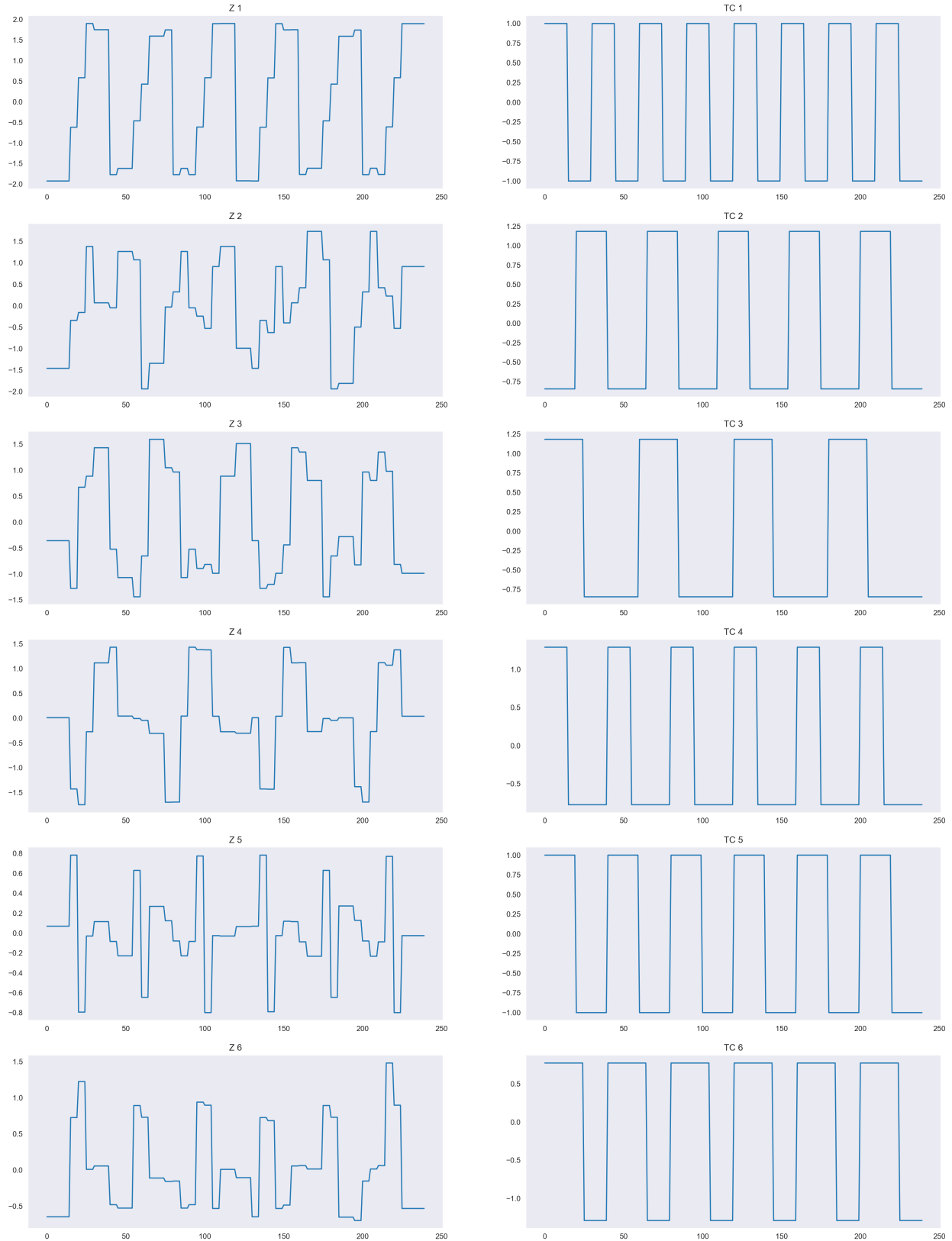


Figure 19: The regressors in \mathbf{Z} and source the TCs

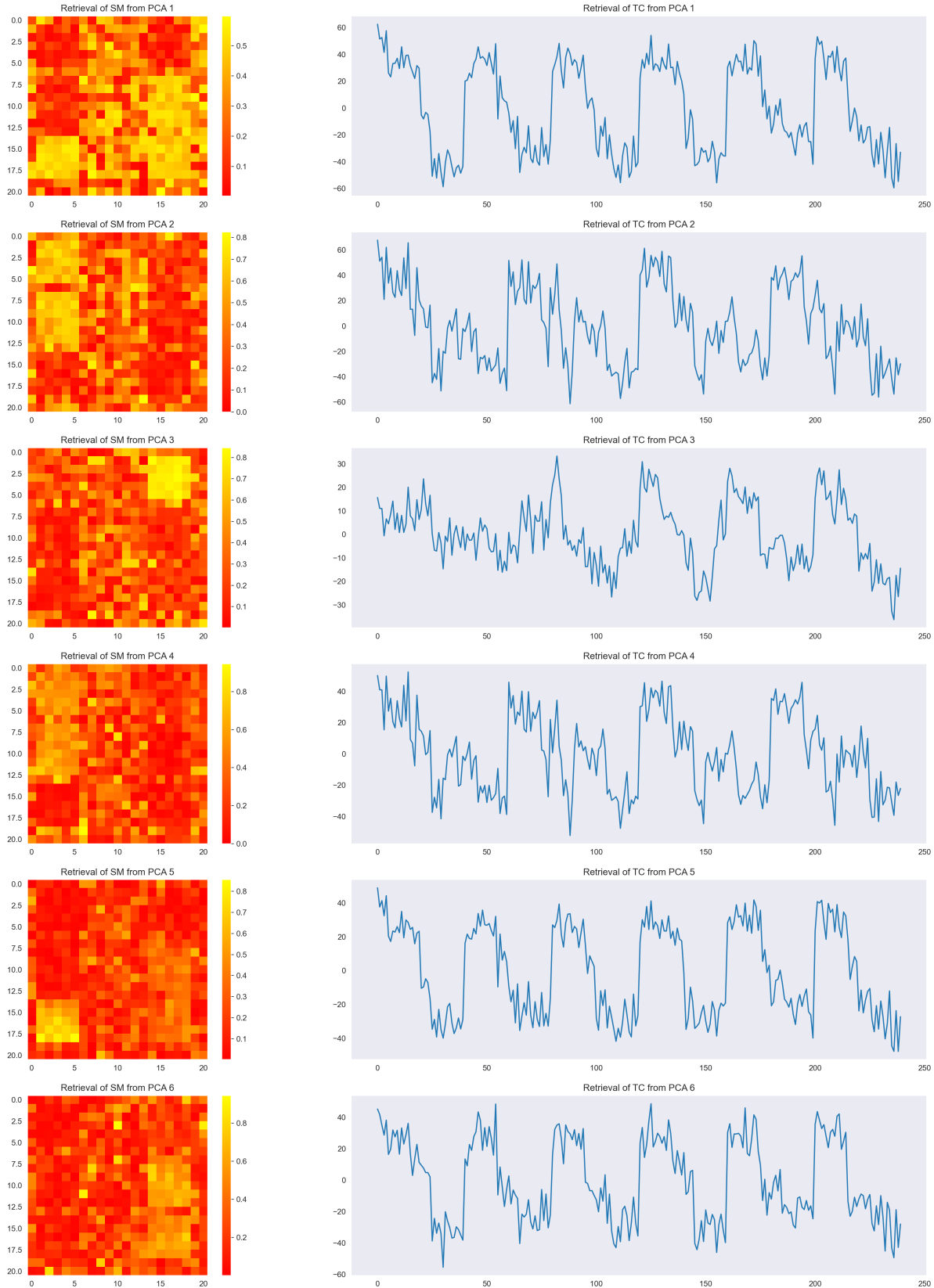


Figure 20: The 6 retrieved sources using LASSO with PCA